Supporting Information

Spectroscopic Analysis of a Library of DNA Tension Probes for Mapping Cellular Forces at Fluid Interfaces

*Roxanne Glazier[1], Pushkar Shinde[2], Hiroaki Ogasawara[2], and Khalid Salaita[1,2]**

[1] Wallace H. Coulter Department of Biomedical Engineering at Georgia Institute of Technology and Emory University. Atlanta, GA. 30322. [2] Emory University Department of Chemistry, Atlanta, GA. 30322.

* Corresponding Author, k.salaita@emory.edu

Table S1 Oligonucleotide Sequences

Purpose	**Sequence**	**Source**
Hairpin Strand (+ Spacers)	GTG AAA TAC CGC ACA GAT GCG TTT GTA TAA ATG TTT TTT TCA TTT ATA C TTT AAG AGC GCC ACG TAG CCC AGC	IDT
Hairpin Strand (- Spacers)	GTG AAA TAC CGC ACA GAT GCG GTA TAA ATG TTT TTT TCA TTT ATA C AAG AGC GCC ACG TAG CCC AGC	IDT
Hairpin (+ Spacers) Complementary Strand	AAA GTA TAA ATG AAA AAA ACA TTT ATA CAA A	IDT
Hairpin (- Spacers) Complementary	GTA TAA ATG AAA AAA ACA TTT ATA C	IDT
5'-Alk-3'-Amine	/5Hexynyl/ TTT GCT GGG CTA CGT GGC GCT CTT /3AmMO/	IDT
5'-Alk-3'-A488	/5Hexynyl/ TTT GCT GGG CTA CGT GGC GCT CTT /3AlexF488N/	IDT
5'-Alk-5T-3'-Amine	/5Hexynyl/ TTT GCT GGG CTA CGT GGC GCT CTT TTT TT /3AmMO/	IDT
5'-Alk-5T-3'-Amine	/5Hexynyl/ TTT GCT GGG CTA CGT GGC GCT CTT TTT TT /3AlexF488N/	IDT
5'-Amine-3'-Biotin	/5AmMC6/CG CAT CTG TGC GGT ATT TCA CTT T/3Bio	IDT
5'-BHQ1-3'-Biotin	BHQ-1-CG CAT CTG TGC GGT ATT TCA CTT T-Biotin	BT
5'-BHQ1-3'	BHQ-1-CG CAT CTG TGC GGT ATT TCA CTT T	BT
5'-9TBHQ1-3'-Biotin	CG CAT CTG-T(BHQ-1)- GC GGT ATT TCA CTT T-Biotin	BT
5'-9TBHQ1-3'	CG CAT CTG -T(BHQ-1)-GC GGT ATT TCA C	BT
5'-9Tamine-Biotin-3'	CGC ATC TG/iAmMC6T/ CGG TAT TTC ACT TT/3Bio/	IDT
5'-Dual Biotin-Hairpin (-Spacers)-3'	/52-Bio/GT GAA ATA CCG CAC AGA TGC GGT ATA AAT GTT TTT TTC ATT TAT ACA AGA GCG CCA CGT AGC CCA GC	IDT

Linear (- Spacers)	GTG AAA TAC CGC ACA GAT GCG AAG AGC GCC ACG TAG CCC AGC	IDT
Linear (+ Spacers)	GTG AAA TAC CGC ACA GAT GCG TTT TTT AAG AGC GCC ACG TAG CCC AGC	IDT

IDT = Integrated DNA Technologies, BT = Biosearch Technologies.

* Note that for synthetic reasons, the biotin modification was moved from the anchor strand to the hairpin strand between single and dual biotin experiments, respectively; we expect this effect to be negligible.

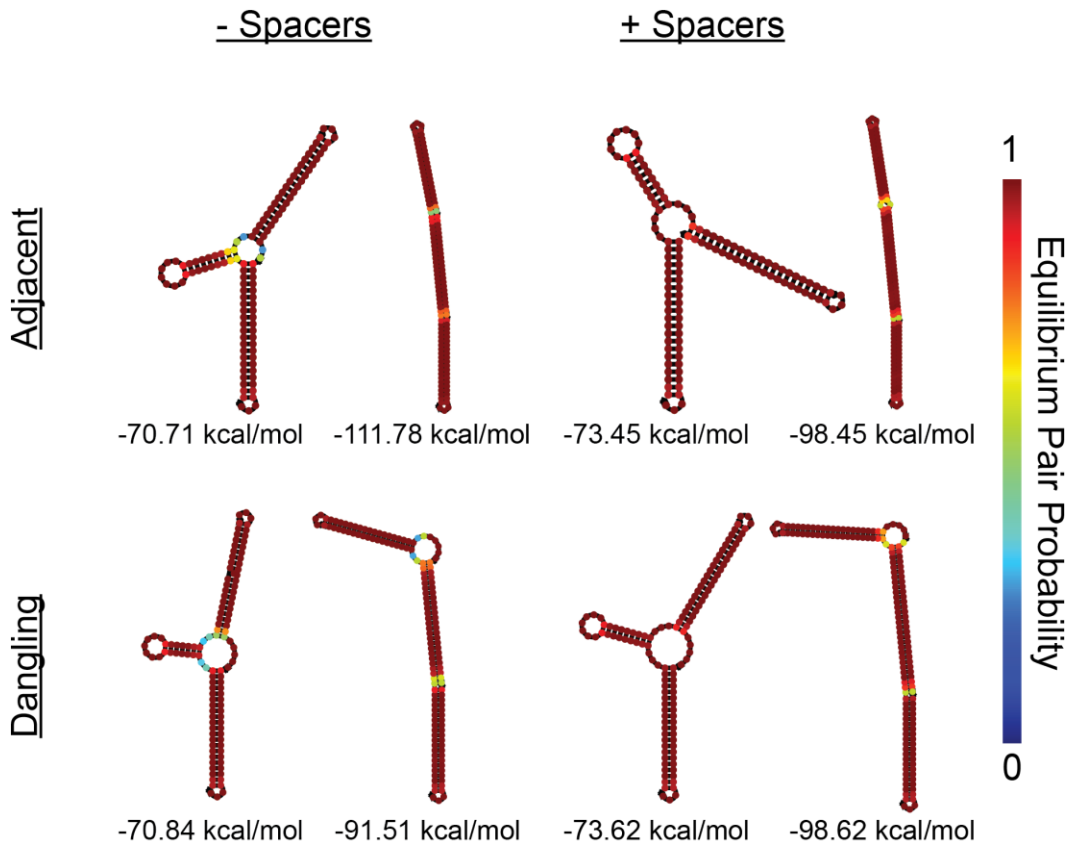

Figure S1 Influence of spacer and overhang sequences on three-way junctions in tension probes.

NUPACK equilibrium pair probability analysis of DNA tension probes in the closed and open conformations. 50 μM probes with 10% excess 'donor strand' were modeled at 25 C in 137 mM NaCl, corresponding to 1x PBS and the approximate conditions for probe incubation on the SLB. The equilibrium pair probability is the probability of base-pairing.

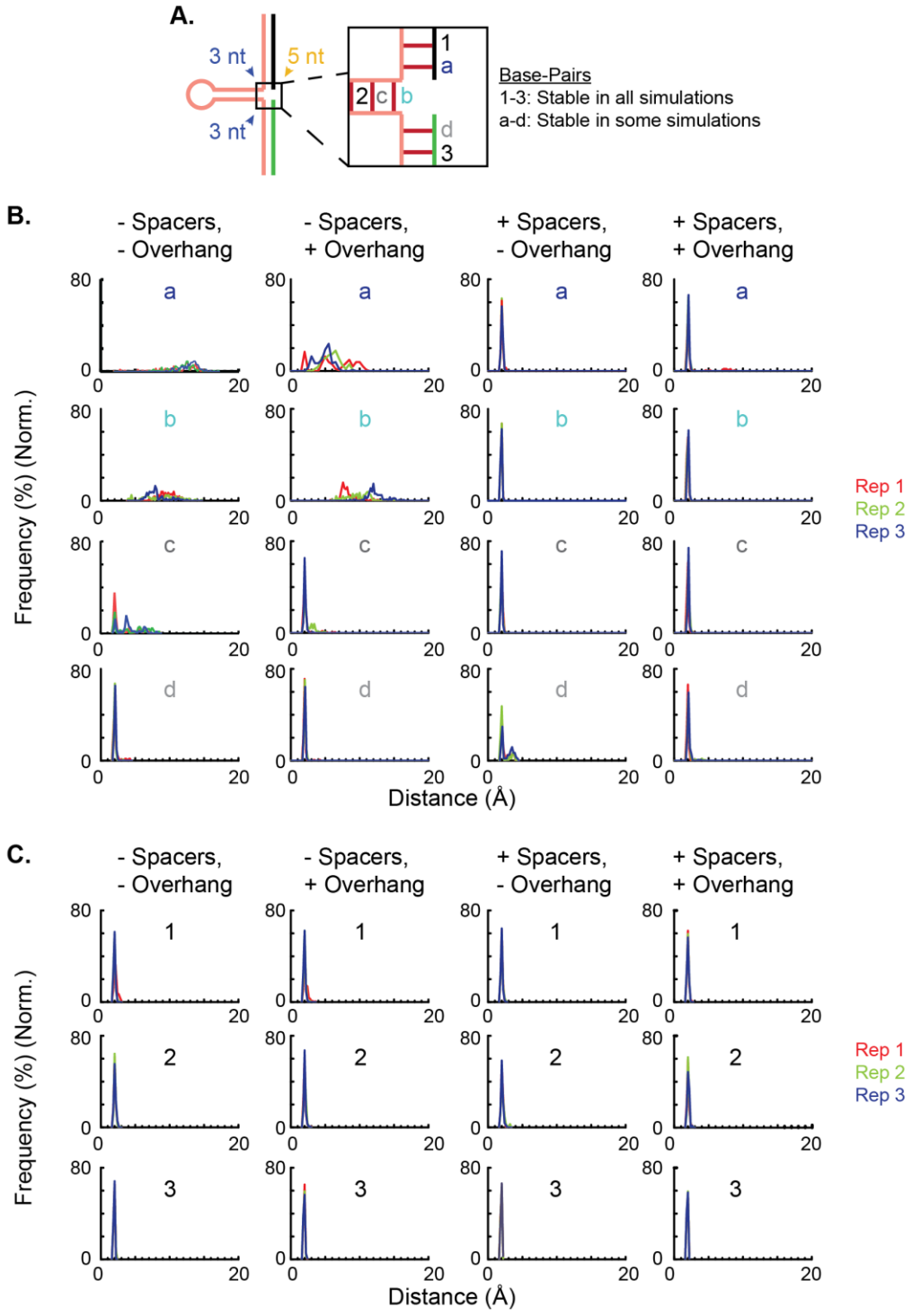

Figure S2 Molecular dynamics simulation results are independent of starting conformation

(A) Graphical schematic of modeled DNA hairpins. Probes were modeled with or without 3T spacers and a 5T overhang. For each hairpin, the distance between the bases was calculated at the sites shown in red, which are labeled a-d or 1-3. BP 1-3 were stable throughout all simulations, whereas BP a-d exhibited fraying in some simulations and conformations. Stable base-pairing is defined as two bases with less than or equal to 2 Å. **(B)** Histogram analysis of distance versus frequency for the indicated DNA bp. BP a-d correspond to the labeled bp in **A**. Individual histogram events quantify distances at simulation snapshots. Traces are coded by simulation, with the first simulation in red, the second in green, and the third in blue. **(C)** Histogram analysis of distance versus frequency for the indicated DNA bp. BP 1-3 correspond to the labeled bp in **A**. Individual histogram events quantify distances at simulation snapshots. Traces are coded by simulation, with the first simulation in red, the second in green, and the third in blue.

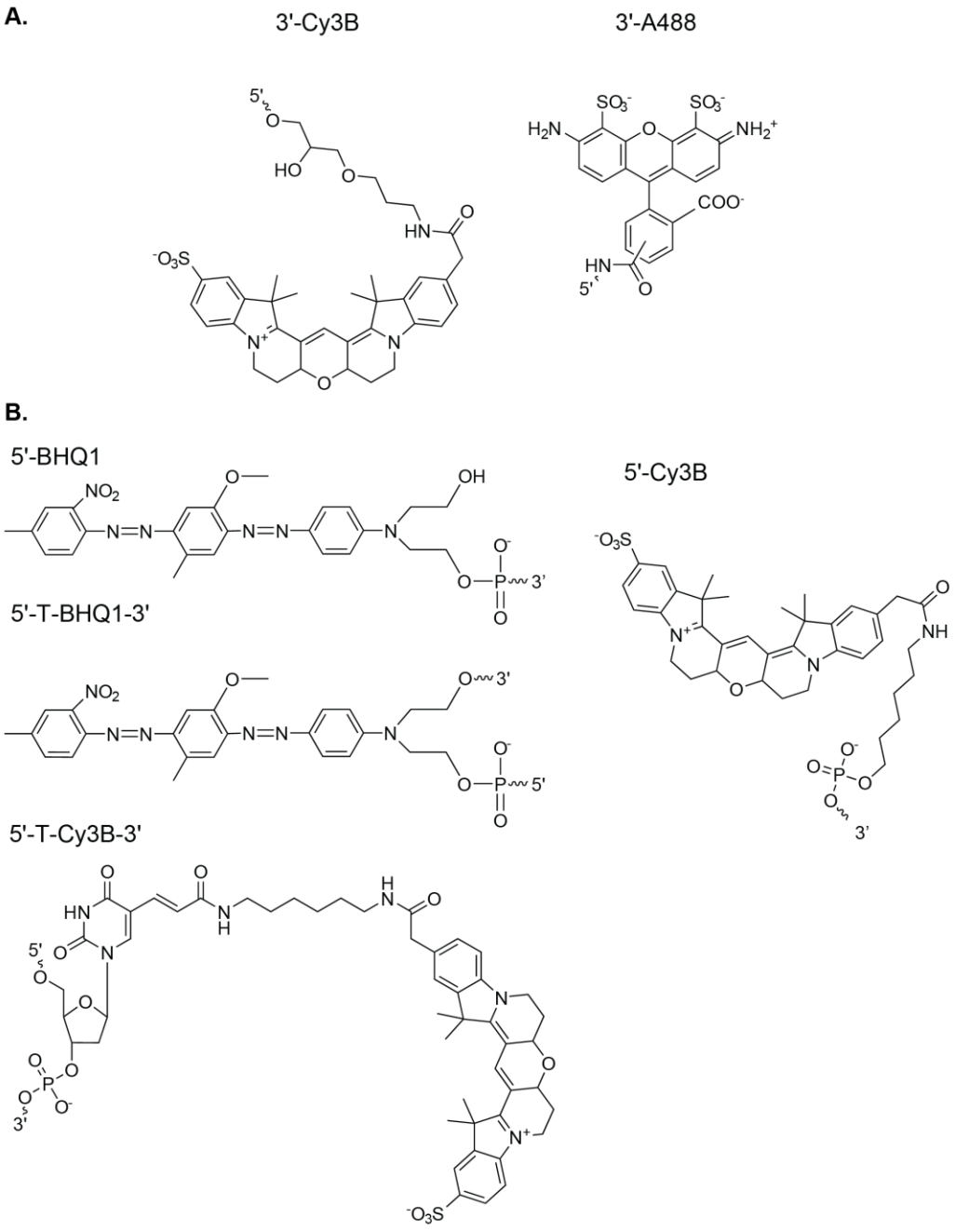

Figure S3 Chemical structures and attachment chemistry for dyes.

Chemical structures for donor **(A)** and acceptor **(B)** dyes and their conjugation chemistry. Dyes attached via a T are incorporated onto a deoxythymidine modification.

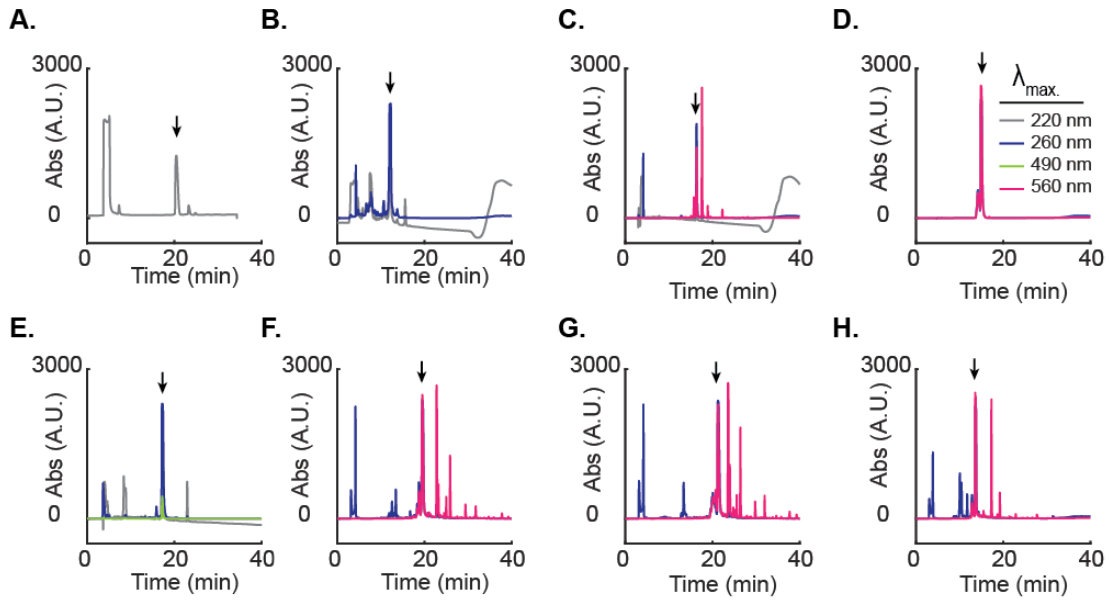

Figure S4 HPLC purification of modified oligonucleotides.

HPLC chromatograms of **(A)** cRGDfk(PEG-PEG)-Azide. **(B)** 5'-cRGDfk(PEG-PEG)- 3'-Amine (intermediate), **(C)** 5'-cRGDfk(PEG-PEG)-3'-Cy3B, **(D)** 5'-Alk-3'-Cy3B, **(E)** 5'-cRGDfk(PEG-PEG) -3'-A488, **(F)** 5'-9TCy3B-3'-Bio, **(G)** 5'-Alk-5T-3'-Cy3B, **(H)** 5'-Cy3B-3'-Bio. Arrows indicate the product peak. D shows a repurified oligonucleotide, due instrument/input error.

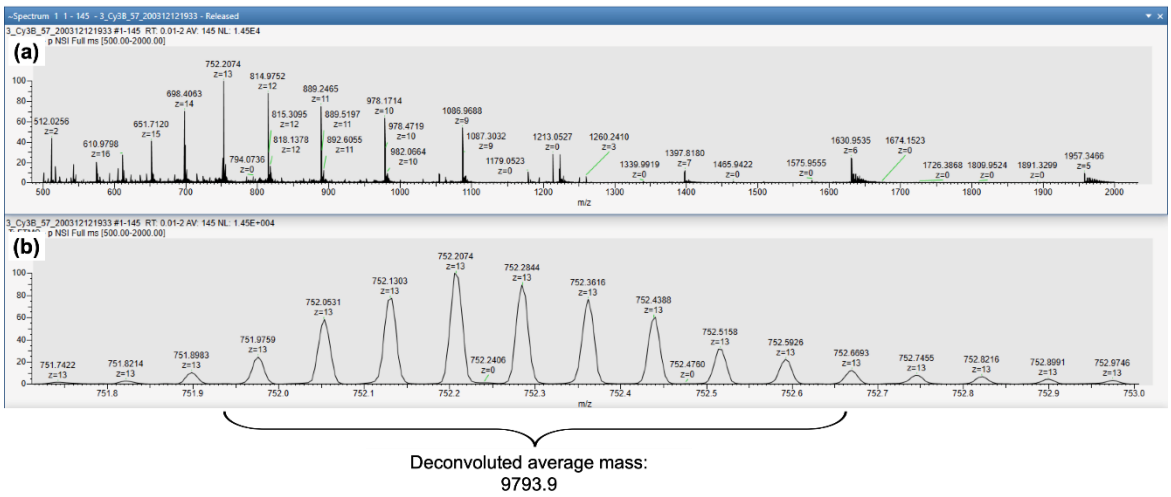

Figure S5 Representative mass spectrometry data.

(**a**) Representative raw mass spectrum. (**b**) Expanded mass spectrum for $z = 13$, with z equal to the ionic valency of the oligonucleotide.

Table S2 Summary of conjugated oligonucleotide mass

Oligonucleotide	**Mass (Expected, Da)**	**Mass (Measured, Da)**
cRGD-5'-3'-A488	9221	9223.1
Cy3B-5'-21-3'-Biotin	8460	8460.6
5'-5T-3'-Cy3B	9792	9793.9
cRGD-5'-3'-Cy3B	9247	9249.3
5'-9T-Cy3B-3'-Biotin	8105	8105.4
5'-Alkyne-3'-Cy3B	8271	8272.4

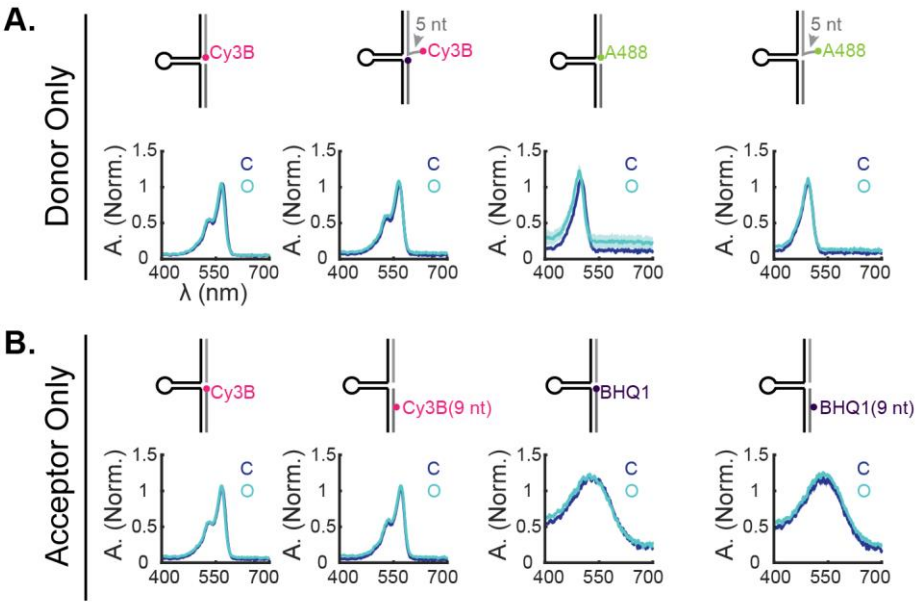

Figure S6 Absorbance spectra of single-dye modified tension probes.

Schematics and absorption spectra of tension probes labeled only with the donor (**A**) or acceptor (**B**). Spectra represent the mean ± s.e.m. for 3 experiments. Outlier spectra (baseline ± 3 median absolute deviations) were omitted.

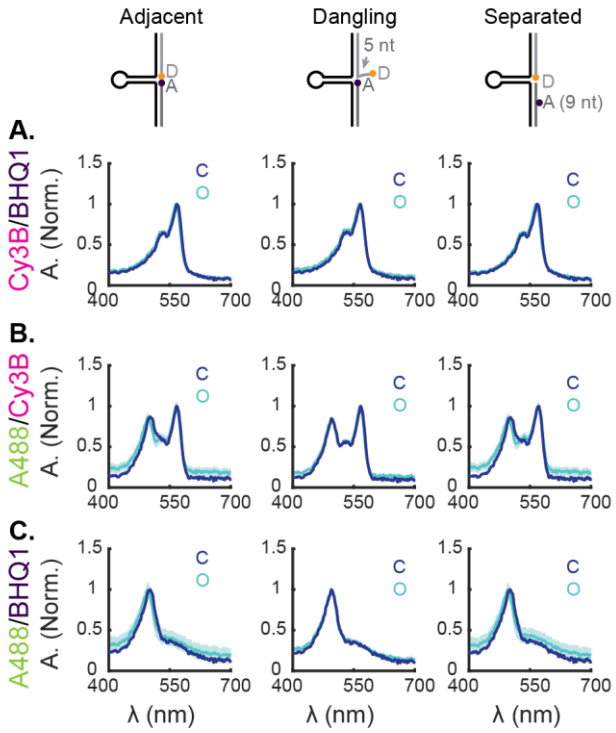

Figure S7 Computed absorbance spectra for tension probes.

Absorbance spectra for (**A**) Cy3B/BHQ1 (**B**) A488/Cy3B and (**C**) A488/BHQ1 probes were calculated by adding absorbance spectra of donor or acceptor only probes (**Figure S6**) normalized by fractional extinction coefficient. Data represent the mean ± s.e.m. and depict the expected signal for pure FRET or DET probes.

Table S3 Absorbance maxima of donor-only probes in-solution.

Cy3B				Cy3B (5 nt)			
Closed		Open		Closed		Open	
$\lambda_{max.}$ (nm)	A (Norm.)	$\lambda_{max.}$ (nm)	A (Norm.)	$\lambda_{max.}$ (nm)	A (Norm.)	$\lambda_{max.}$ (nm)	A (Norm.)
-	-	527	0.54	527	0.55	527	0.6
533	0.54	533	0.56	533	0.57	534	0.61
537	0.54	537	0.55	538	0.55	538	0.6
569	1.05	567	1.06	567	1.06	565	1.09
A488				**A488 (5 nt)**			
Closed		**Open**		**Closed**		**Open**	
$\lambda_{max.}$ (nm)	A (Norm.)	$\lambda_{max.}$ (nm)	A (Norm.)	$\lambda_{max.}$ (nm)	A (Norm.)	$\lambda_{max.}$ (nm)	A (Norm.)
-	-	496	1.22	495	1.08	495	1.13
502	1.1	-	-	-	-	-	-

Table S4 Absorbance maxima of acceptor-only probes in-solution.

Cy3B				Cy3B (9 nt)			
Closed		Open		Closed		Open	
$\lambda_{max.}$ (nm)	A (Norm.)	$\lambda_{max.}$ (nm)	A (Norm.)	$\lambda_{max.}$ (nm)	A (Norm.)	$\lambda_{max.}$ (nm)	A (Norm.)
n/a	n/a	527	0.55	n/a	n/a	n/a	n/a
533	0.54	533	0.56	534	0.55	534	0.59
537	0.54	537	0.55	537	0.56	538	0.6
569	1.05	567	1.06	572	1.04	571	1.07
BHQ1				**BHQ1 (9 nt)**			
Closed		**Open**		**Closed**		**Open**	
$\lambda_{max.}$ (nm)	A (Norm.)	$\lambda_{max.}$ (nm)	A (Norm.)	$\lambda_{max.}$ (nm)	A (Norm.)	$\lambda_{max.}$ (nm)	A (Norm.)
n/a	n/a	n/a	n/a	533	0.568	533	0.57
535	1.12	537	1.26	537	0.561	537	0.56
n/a	n/a	n/a	n/a	568	1.05	567	1.07

Table S5 Absorbance maxima of DNA-based force probes in-solution.

A_Cy3B/BHQ1				**D_Cy3B/BHQ1**				**S_Cy3B/BHQ1**			
Closed		**Open**		**Closed**		**Open**		**Closed**		**Open**	
λ_{max}	**A**	**λ_{max}**	**A**	**λ_{ma}**	**A**	**λ_{max}**	**A**	**$\lambda_{max.}$**	**A**	**$\lambda_{max.}$**	**A**
528	1.01	528	0.67	528	0.99	528	0.71	528	0.64	528	0.64
534	1.04	533	0.68	534	1.03	533	0.73	534	0.67	533	0.66
566	0.86	566	1.03	566	0.92	566	1.05	569	1.03	567	1.04
A_A488/Cy3B				**D_A488/Cy3B**				**S_A488/Cy3B**			
Closed		**Open**		**Closed**		**Open**		**Closed**		**Open**	
λ_{max}	**A**	**λ_{max}**	**A**	**λ_{max}**	**A**	**λ_{max}**	**A**	**$\lambda_{max.}$**	**A**	**$\lambda_{max.}$**	**A**
496	0.71	496	0.77	496	0.76	496	0.78	n/a	n/a	496	0.84
501	0.71	-	-	-	-	-	-	503	0.75	-	-
528	0.56	527	0.58	528	0.55	527	0.57	528	0.54	534	0.59
533	0.56	533	0.58	533	0.56	533	0.57	534	0.56	537	0.6
537	0.55	-	-	-	-	-	-	537	0.56	-	-
567	1.02	566	1.08	567	1.01	567	1.06	571	1.02	571	1.07
A_A488/BHQ1				**D_A488/BHQ1**				**S_A488/BHQ1**			
Closed		**Open**		**Closed**		**Open**		**Closed**		**Open**	
λ_{max}	**A**	**λ_{max}**	**A**	**λ_{max}**	**A**	**λ_{max}**	**A**	**$\lambda_{max.}$**	**A**	**$\lambda_{max.}$**	**A**
496	1.01	495	1.14	495	1.04	496	1.08	-	-	495	1.15
500	1.02	-	-	499	1.02	-	-	503	1.05	-	-

λ_{max} is reported in nm; A is normalized.

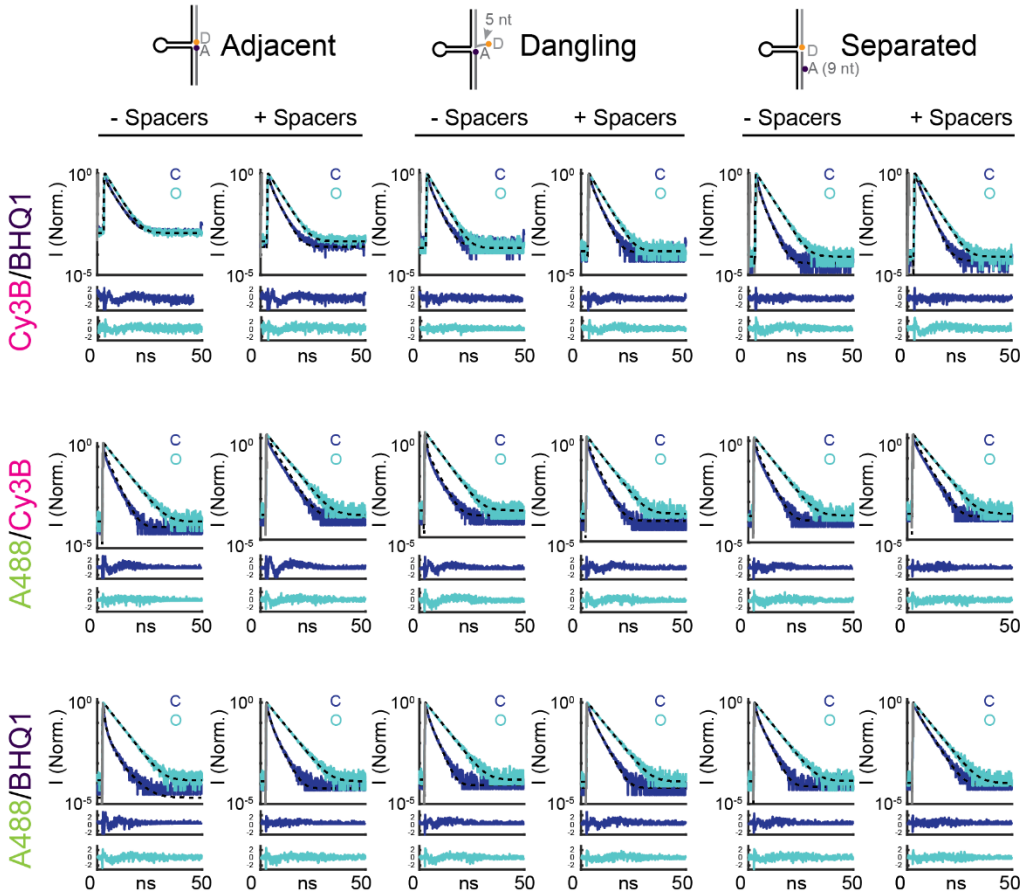

Figure S8 Representative TCSPC decay curves and fits

Representative TCSPC decay curves and curve fits (dashed black lines) and residuals for closed and open tension probes on SLBs. Probes were fit in SymPhoTime as described in the methods section using the system IRF (grey). For visualization, curves are averaged over 5 time-bin windows. Open probes were fit to a monoexponential decay. Closed probes were fit to a bi- or triexponential decay. For all curves, $\chi^2 < 2$.

Table S6 Summary of SLB fluorescence intensity and quenching efficiency

Probe		Closed (A.U.)	Open (A.U.)	QE (%)
Cy3B/BHQ1	***A_Cy3B/BHQ1-**	56 ± 11	5210 ± 307	99 ± 1
	***A_Cy3B/BHQ1+**	102 ± 10	6030 ± 351	98 ± 0
	D_Cy3B/BHQ1-	66 ± 8	3594 ± 298	98 ± 0
	D_Cy3B/BHQ1+	132± 24	2736 ± 311	94 ± 2
	S_Cy3B/BHQ1-	655 ± 25	2988 ± 71	78 ± 3
	S_Cy3B/BHQ1+	1156 ± 45	2367 ± 121	51 ± 4
A488/Cy3B	**A_A488/Cy3B-**	80 ± 4	2153 ± 107	96 ± 1
	A_A488/Cy3B+	195 ± 49	1785 ± 122	89 ± 5
	D_A488/Cy3B-	344 ± 31	2186 ± 147	84 ± 7
	D_A488/Cy3B+	475 ± 97	1788 ± 258	74 ± 7
	S_A488/Cy3B-	379 ± 15	2046 ± 268	78 ± 14
	S_A488/Cy3B+	735 ± 43	2021 ± 205	48 ± 1
A488/BHQ1	**A_A488/BHQ1-**	92 ± 8	1847 ± 171	95 ± 1
	A_A488/BHQ1+	262 ± 25	1668 ± 228	84 ± 4
	D_A488/BHQ1-	557 ± 44	2177 ± 274	73 ± 10
	D_A488/BHQ1+	671 ± 62	2038 ± 130	67 ± 7
	S_A488/BHQ1-	592 ± 21	2757 ± 220	78 ± 5
	S_A488/BHQ1+	740 ± 169	2087 ± 177	65 ± 5

* A_Cy3B/BHQ1 SLBs were prepared using 0.2 mol % biotinyl-cap PE. All other SLBs for spectroscopic analysis (cell-free) were prepared with 0.1 mol % biotinyl-cap PE. Intensity data represent the mean ± s.e.m. of at least 3 experiments per condition. QE represents the mean ± s.d. of at least 3 experiments per condition.

Table S7 Summary of SLB-bound probe fluorescence lifetime, τ

Probe		$\tau_{Av\ FAST}$ (ns)		$\tau_{Av\ \ Int.}$(ns)		$\tau_{Av\ Amp.}$ (ns)		
		Closed	**Open**	**Closed**	**Open**	**Closed**	**Open**	**QE (%)**
Cy3B/BHQ1	***A_Cy3B/BHQ1-**	2.388 ± 0.428 (0.076)	2.592 ± 0.325 (0.220)	2.305 ± 0.086	2.602 ± 0.012	1.760 ± 0.188	2.566 ± 0.037	31 ± 18
	***A_Cy3B/BHQ1+**	1.685 ± 0.251 (0.036)	2.589 ± 0.296 (0.037)	1.612 ± 0.018	2.614 ± 0.009	1.092 ± 0.015	2.621 ± 0.009	58 ± 2
	D_Cy3B/BHQ1-	1.777 ± 0.500 (0.110)	2.405 ± 0.554 (0.051)	1.753 ± 0.124	2.481 ± 0.001	1.328 ± 0.112	2.481 ± 0.000	46 ± 7
	D_Cy3B/BHQ1+	1.654 ± 0.199 (0.028)	2.574 ± 0.279 (0.010)	1.595 ± 0.124	2.523 ± 0.004	1.245 ± 0.042	2.523 ± 0.004	51 ± 3
	S_Cy3B/BHQ1-	1.089 ± 0.149 (0.017)	2.659 ± 0.319 (0.014)	1.099 ± 0.009	2.693 ± 0.007	0.743 ± 0.008	2.693 ± 0.007	72 ± 1
	S_Cy3B/BHQ1+	1.626 ± 0.208 (0.006)	2.625 ± 0.324 (0.056)	1.670 ± 0.010	2.633 ± 0.044	1.432 ± 0.012	2.634 ± 0.044	46 ± 3
A488/Cy3B	**A_A488/Cy3B-**	1.349 ± 0.465 (0.132)	3.003 ± 0.712 (0.067)	1.546 ± 0.073	3.061 ± 0.001	0.418 ± 0.034	3.061 ± 0.009	84 ± 2
	A_A488/Cy3B+	1.214 ± 0.164 (0.059)	3.292 ± 0.332 (0.085)	1.151 ± 0.012	3.233 ± 0.008	0.688 ± 0.026	3.233 ± 0.009	78 ± 1
	D_A488/Cy3B-	1.132 ± 0.170 (0.035)	3.093 ± 0.372 (0.042)	1.106 ± 0.036	3.084 ± 0.0146	0.713 ± 0.026	3.084 ± 0.015	77 ± 2
	D_A488/Cy3B+	1.434 ± 0.262 (0.077)	3.243 ± 0.406 (0.014)	1.418 ± 0.082	3.255 ± 0.008	1.002 ± 0.113	3.255 ± 0.008	69 ± 7
	S_A488/Cy3B-	1.520 ± 0.207 (0.021)	3.361 ± 0.307 (0.032)	1.507 ± 0.016	3.346 ± 0.089	1.005 ± 0.013	3.345 ± 0.009	69 ± 1
	S_A488/Cy3B+	2.166 ± 0.208 (0.011)	3.396 ± 0.288 (0.014)	2.189 ± 0.015	3.423 ± 0.010	1.788 ± 0.018	3.423 ± 0.010	69 ± 1
A488/BHQ1	**A_A488/BHQ1-**	0.943 ± 0.181 (0.043)	3.180 ± 0.343 (0.037)	1.546 ± 0.073	3.061 ± 0.009	0.440 ± 0.016	3.244 ± 0.015	86 ± 1
	A_A488/BHQ1+	1.278 ± 0.187 (0.030)	3.31 ± 0.365 (0.047)	1.151 ± 0.012	3.233 ± 0.009	0.828 ± 0.007	3.400 ± 0.014	76 ± 0
	D_A488/BHQ1-	1.300 ± 0.200 (0.026)	3.349 ± 0.389 (0.011)	1.106 ± 0.036	3.084 ± 0.015	0.956 ± 0.003	3.311 ± 0.008	71 ± 0
	D_A488/BHQ1+	1.781 ± 0.239 (0.038)	3.361 ± 0.390 (0.013)	1.418 ± 0.082	3.255 ± 0.008	1.410 ± 0.016	3.429 ± 0.009	59 ± 1
	S_A488/BHQ1-	1.503 ± 0.263 (0.040)	3.3340 ± 0.356 (0.022)	1.507 ± 0.016	3.346 ± 0.009	1.064 ± 0.005	3.388 ± 0.007	69 ± 0
	S_A488/BHQ1+	2.261 ± 0.386 (0.031)	3.418 ± 0.475 (0.016)	2.189 ± 0.015	3.423 ± 0.010	1.874 ± 0.016	3.429 ± 0.007	45 ± 1

* A_Cy3B/BHQ1 SLBs were prepared using 0.2 mol % biotinyl-cap PE. All other SLBs were prepared with 0.1 mol % biotinyl-cap PE. $\tau_{Av\ Amp}$ and $\tau_{Av\ Int}$ represent the mean ± s.e.m. of at least 3 experiments per condition. For $\tau_{Av\ FAST}$, error reflects the histogram width, and s.e.m. is shown in parentheses. Here, QE represents the mean ± s.d. of at least 3 experiments per condition calculated using $\tau_{Av\ Amp}$.

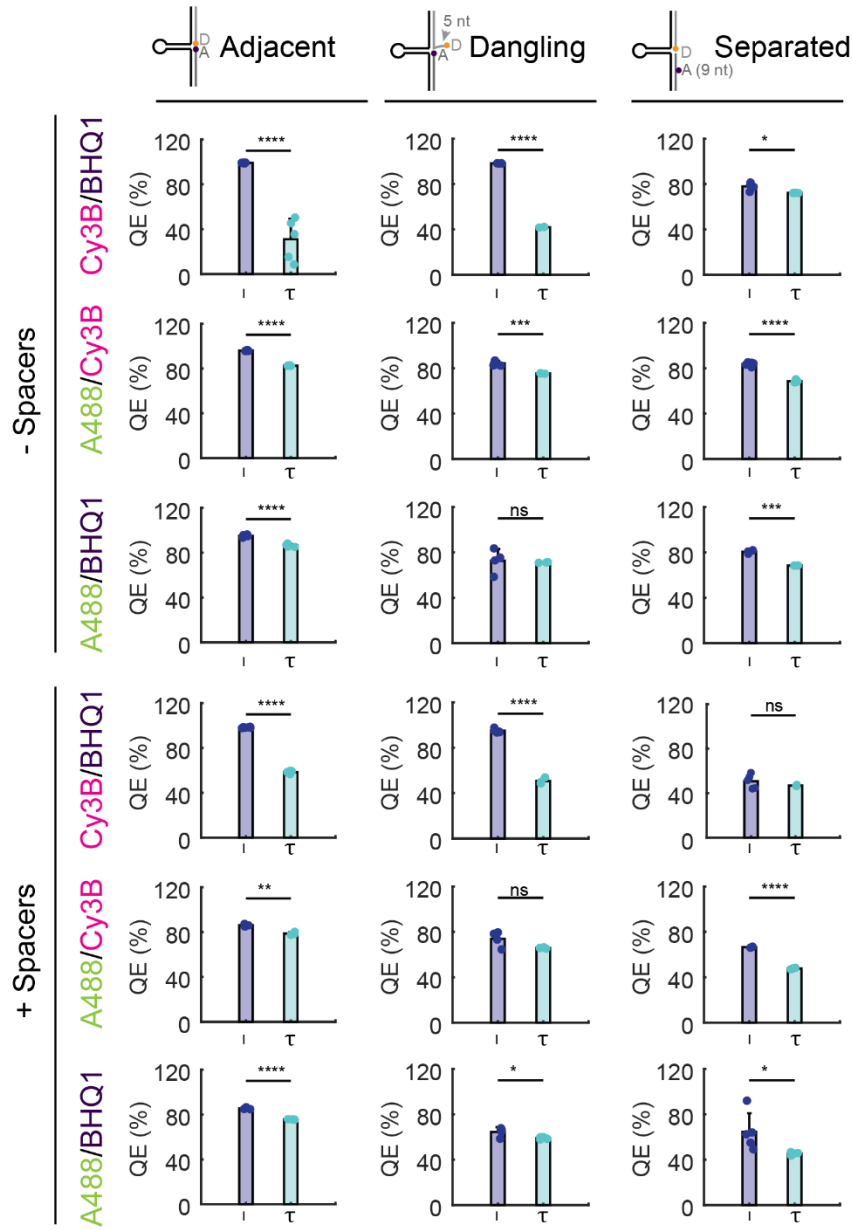

Figure S9 Analysis of intensity and lifetime derived quenching efficiencies.

Scatter plots of quenching efficiencies calculated using the fluorescence intensity (I) versus the amplitude-average lifetime ($\tau_{Av\ Amp}$). Bars and error bars represent the mean ± SD for at least 3 experiments. Outliers beyond 3 median absolution deviations were omitted. Statistics were performed using a two-tailed unpaired T-test. P values are reported as ns P>0.05, *P < 0.05, **P < 0.01, ***P < 0.0001, **** P < 0.0001.

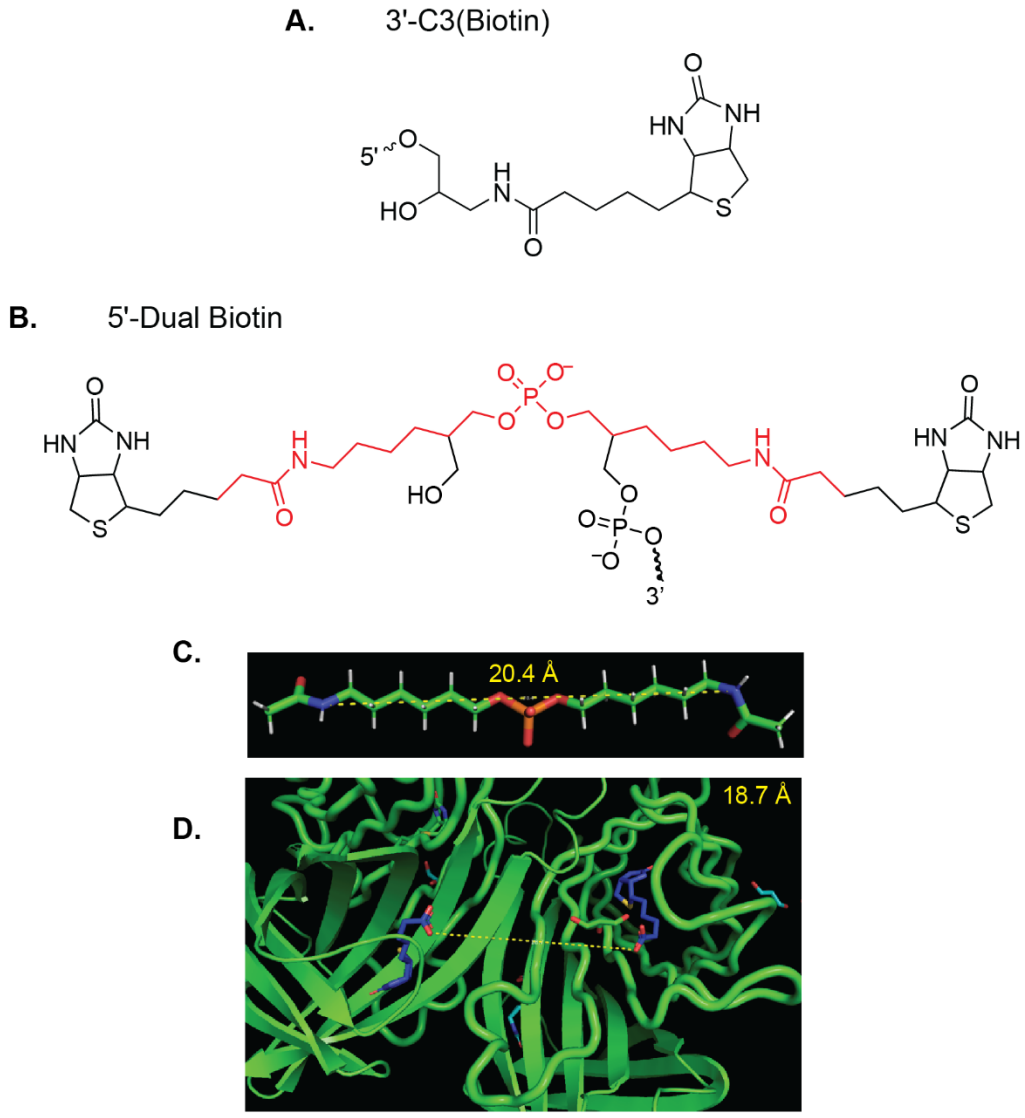

Figure S10 Structural analysis of biotin and streptavidin

(A) Chemical structure of 3' Biotin (Biosearch Technologies). **(B)** Chemical structure of 5'-Dual Biotin (Integrated DNA Technologies). The region in red was modeled in WebMO to determine its 3D end-to-end distance. **(C)** 3D model of the dual biotin linker. The yellow dashed line was used to measure the end-to-end distance. **(D)** 3D crystal structure of streptavidin with bound biotin molecules. The yellow dashed line was used to determine the distance between biotin-binding sites.

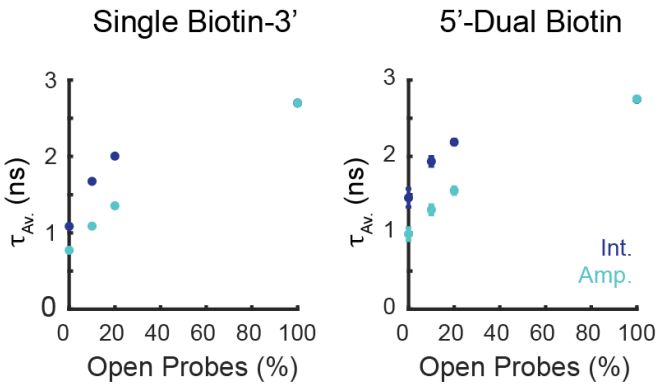

Figure S11 S_Cy3B/BHQ1- fluorescence lifetimes as a function of open probe density and probe biotinylation

Average $\tau_{Av\ Int}$ (dark blue) and $\tau_{Av\ Amp}$ (light teal) for SLBs containing S_Cy3B/BHQ1- probes anchored with a single or dual biotin. Data represent the mean ± s.e.m of 3 experiments. All SLBs containing closed probes displayed multiple lifetime components regardless of probe biotinylation.

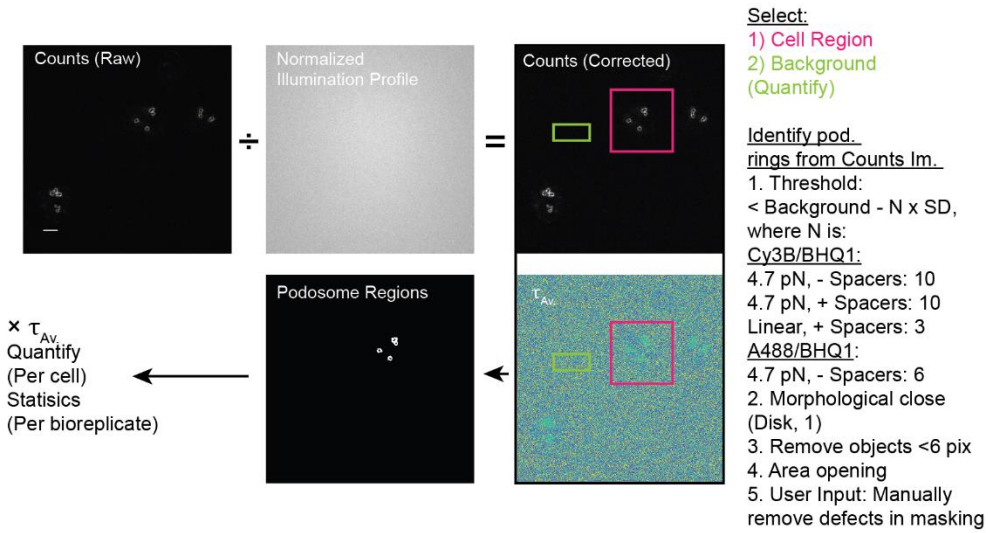

Figure S12 Analysis map for podosome identification on high QE probes

The FLIM photon counts image was illumination profile corrected and used to select regions of interest containing a podosome-forming cell and the SLB background. Podosomes were detected by the presence of bright rings in the photon counts image. Scale bar, 5 μm.

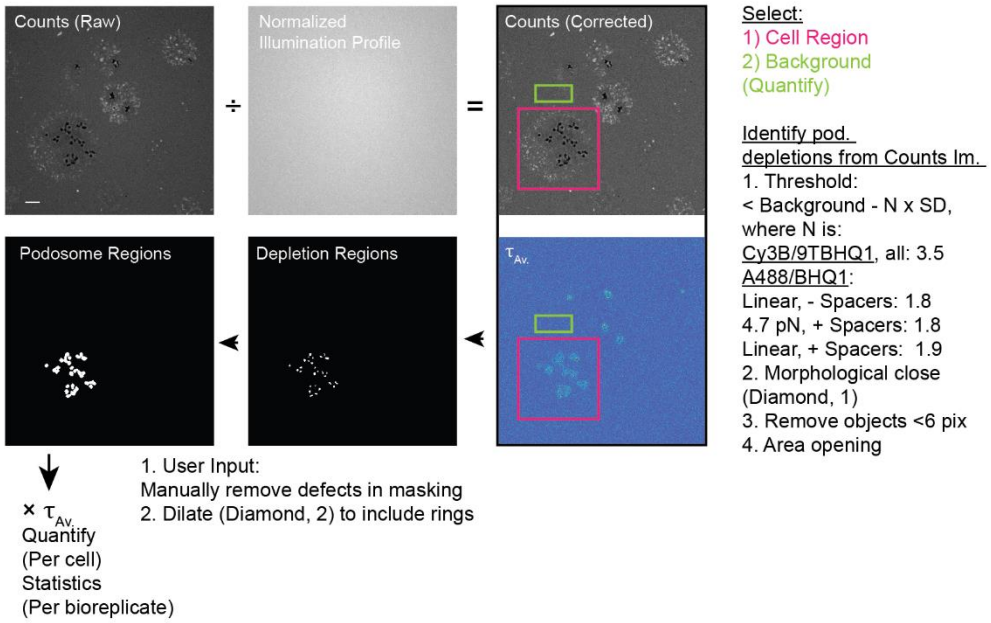

Figure S13 Analysis map for podosome identification on low QE probes

The FLIM photon counts image was illumination profile corrected and used to select regions of interest containing a podosome-forming cell and the SLB background. Podosomes were detected based on the decrease in fluorescence intensity at the podosome cores and rings were included through mask dilation. Scale bar, 5 μm.

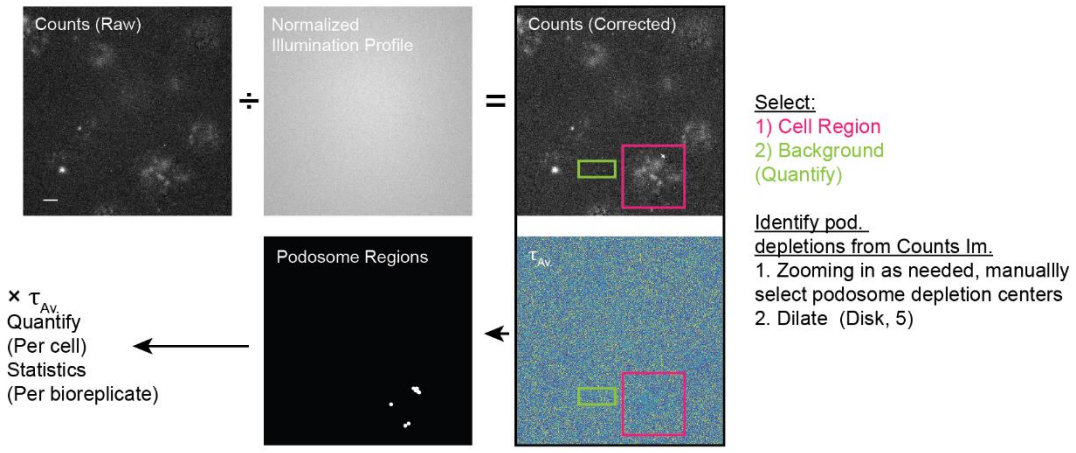

Figure S14 Analysis map for podosome identification on A_Cy3B/BHQ1- Linear probes

The FLIM photon counts image was illumination profile corrected and used to select regions of interest containing a podosome-forming cell and the SLB background. Individual podosome depletion regions were hand-selected and pixels were dilated to include the entire podosome region. Scale bar, 5 μm.

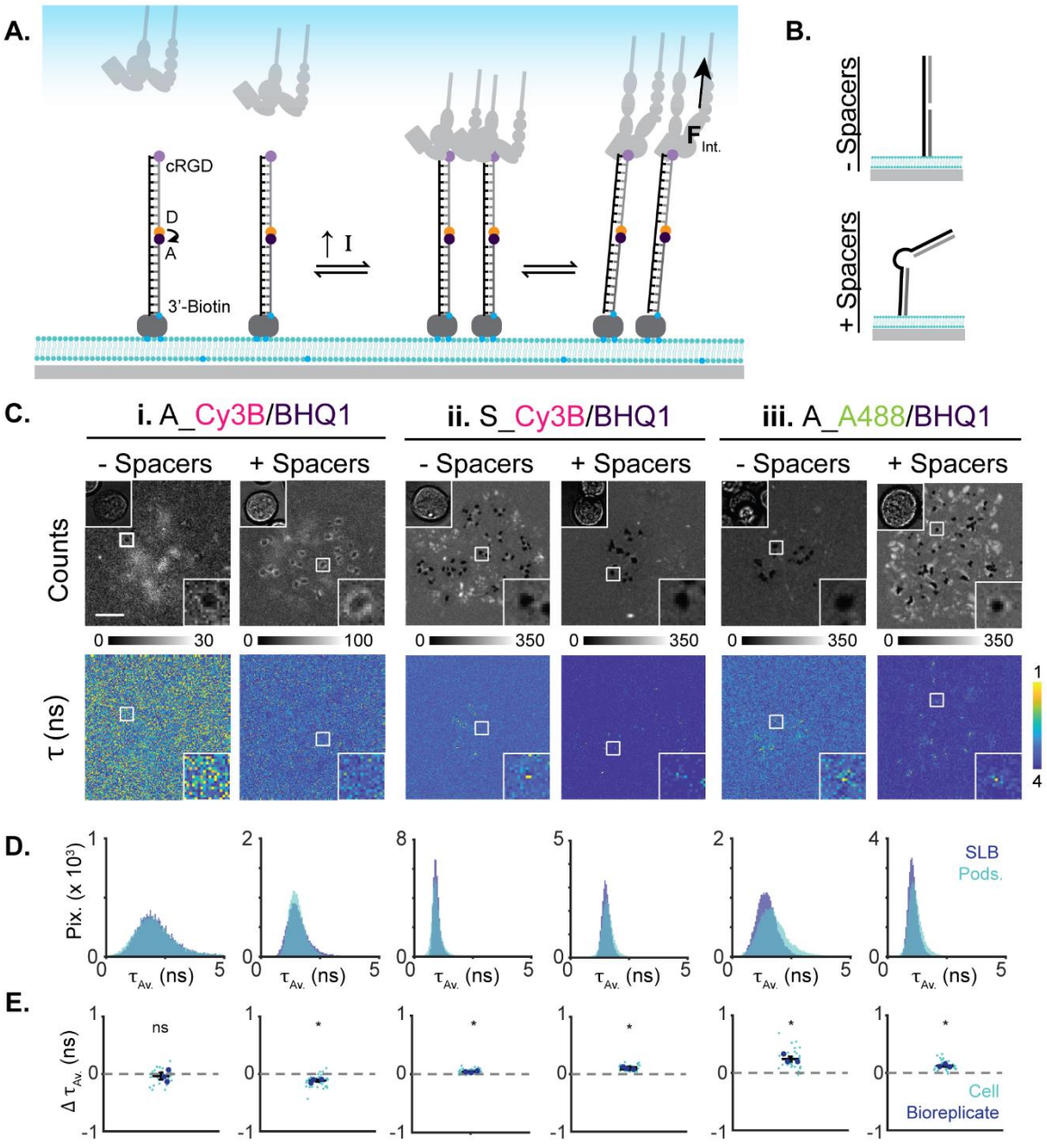

Figure S15 Tension signal is primarily contributed by hairpin unfolding.

(A) Schematic of linear control probes, which lack a stem-loop sequence and cannot mechanically unfold. Probes may be transported on the SLB, leading to a change in intensity, but even under cellular forces, oligos cannot unfold. **(B)** Linear control probes mimicked tension probes but lacked a stem-loop sequence. Backbone spacer sequences were incorporated as indicated. **(C)**

Representative fluorescence micrographs of NIH 3T3 cells forming podosomes on SLBs with linear probes. Transmitted images are shown in the upper left of the corner of the Counts image. White boxes indicate zoom-in regions shown in the lower right corner. **(D)** Histogram analysis of the images shown above in C. For each probe, N random pixels were selected in the SLB background, where N was the number of pixels in the podosome region. **(E)** Quantification of the change in $\Delta\tau_{Av\ FAST}$ on the 6 evaluated tension probes. Small teal markers represent data points from individual cells; large blue markers represent the mean per bioreplicate. Error bars represent the mean ± s.e.m. A two-tailed t-test was used to determine whether the mean was significantly different than zero. Experiments were repeated at least 3 times. Significance is as indicated, with ns, P > 0.05, *, P < 0.05 , and **, P < 0.01. Scale bar, 5 μm.

Table S8 Estimated tension probe $F_{1/2}$ thresholds

Frayed BP	Effective Stem-Loop Sequence	Bases	ΔG_{Unfold} (J/molecule)	$\Delta G_{Stretch}$ (J/molecule)	ΔG_{Total} (J/molecule)	$F_{1/2}$ (pN)
0	GTA TAA ATG TTT TTT TCA TTT ATA C	25	3.55E-20	1.54E-20	5.09E-20	5.9
1	TA TAA ATG TTT TTT TCA TTT ATA	23	2.84E-20	1.32E-20	4.17E-20	5.4
2*	A TAA ATG TTT TTT TCA TTT AT	21	2.42E-20	1.21E-20	3.54E-20	5.2
2	A TAA ATG TTT TTT TCA TTT AT	21	1.99E-20	1.21E-20	3.11E-20	4.6

* Additional secondary structure predicted by IDT's OligoAnalyzer Tool for 1 frayed bp input